Geology

Polygonal faults in chalk: Insights from extensive exposures of the Khoman Formation, Western Desert, Egypt

Barbara J. Tewksbury, John P. Hogan, Simon A. Kattenhorn, Charlotte J. Mehrtens and Elhamy A. Tarabees

Geology 2014;42;479-482
doi: 10.1130/G35362.1

Notes

Polygonal faults in chalk: Insights from extensive exposures of the Khoman Formation, Western Desert, Egypt

Barbara J. Tewksbury[1], John P. Hogan[2], Simon A. Kattenhorn[3], Charlotte J. Mehrtens[4], and Elhamy A. Tarabees[5]
[1]Department of Geosciences, Hamilton College, Clinton, New York 13323, USA
[2]Geology and Geophysics Program, Missouri University of Science and Technology, Rolla, Missouri 65409, USA
[3]Department of Geological Sciences, University of Idaho, Moscow, Idaho 83844, USA
[4]Department of Geology, University of Vermont, Burlington, Vermont 05405, USA
[5]Department of Geology, Damanhour University, Damanhour 22516, Egypt

ABSTRACT

Although polygonal fault systems and related features are common in fine-grained sediments in modern submarine basins and have been studied in basins worldwide using three-dimensional (3-D) seismic data, extensive on-land exposures have remained elusive. We report here on the discovery of a polygonal fault system occurring in nearly continuous surface exposure over ~900 km^2 in chalk of the Cretaceous Khoman Formation near Farafra Oasis, Egypt. Field exposures reveal polygon boundaries defined by clusters of dozens of normal faults with strongly grooved fault surfaces and coarse calcite veins along faults with evidence for multiple fluid flow events. Geometric patterns and fault intersections reveal that mechanically interacting normal faults with multiple orientations were active contemporaneously in a horizontal strain field that was essentially isotropic and extensional. We interpret the very steep dips (~80°) to reflect fault initiation in response to elevated pore fluid pressures. In the uppermost part of the Khoman Formation, a terrain of isolated circular structures displaying shallow inward dips overlies the polygonal fault network. The spatial relationship to the underlying faults is consistent with these small circular basins having formed as fluid escape structures as the polygonal fault system evolved. Outcrops in the Khoman Formation provide an unprecedented look into the 3-D geometry of a polygonal fault system, providing context for the analysis of analogous systems in marine basins and other on-land exposures.

INTRODUCTION

The formation of layer-bound normal faults and shear fractures arrayed in broadly polygonal networks is recognized as a common occurrence during the early burial history and diagenesis of very fine-grained sedimentary sequences. Over the past 20 years, polygonal fault systems have been discovered using two- and three-dimensional (2-D and 3-D) seismic data in >100 sedimentary basins worldwide, almost exclusively in the subsurface in marine settings on continental margins (Cartwright, 2011).

Despite the fact that polygonal fault systems are remarkably common in modern and ancient marine basins, few on-land exposures have been documented that lend themselves to field study. Polygonal faults have been proposed to occur in Paleogene claystones in Belgium (Verschuren, 1992) and in discontinuous, widely separated outcrops and quarry exposures of Cretaceous chalk in the UK and France (Hibsch et al., 2003).

Chalk of the Khoman Formation near Farafra Oasis, Egypt (Fig. 1), contains thousands of narrow, low-relief ridges exposed nearly continuously over a minimum of 900 km^2 and extending, partly mantled by eolian sand, over at least 1800 km^2. Our work with high-resolution satellite imagery shows that these ridges are arrayed in a polygonal network with geometries and scales similar to those of polygonal faults studied using 3-D seismic data. Our field analysis has documented an extensive tract of polygonal faults and related features, allowing us to characterize the 3-D architecture of a polygonal fault system in chalk, small-scale fault zone features, the formation mechanics, and the role of fluids in fault system evolution.

POLYGONAL FAULT SYSTEMS

Polygonal fault systems consist of an array of layer-bound normal faults that partially or fully intersect in broadly polygonal patterns. Faults of different orientations in a polygonal system have been suggested to form synchronously in an essentially isotropic horizontal stress field ($S_{hmax} = S_{hmin}$) (Cartwright and Dewhurst, 1998; Cartwright et al., 2003; Hibsch et al., 2003; Gay et al., 2004; Cartwright, 2011). Although strains are radially isotropic and extensional, layers containing polygonal faults are suggested to have undergone no net extension because host rocks undergo simultaneous volume loss accompanied by fluid expulsion. As the layer shrinks radially, polygonal networks of small-scale and meso-scale normal faults develop.

Polygonal faults form early in the burial history of fine-grained sediments. Although the vast majority previously described occur in clay-rich sediments, polygonal fault systems have been reported in chalk (Hibsch et al., 2003; Hansen et al., 2004). Faults extend nearly to the seafloor in some systems, and polygonal fault systems continue to develop as burial increases, with compaction-induced rotation resulting in shal-

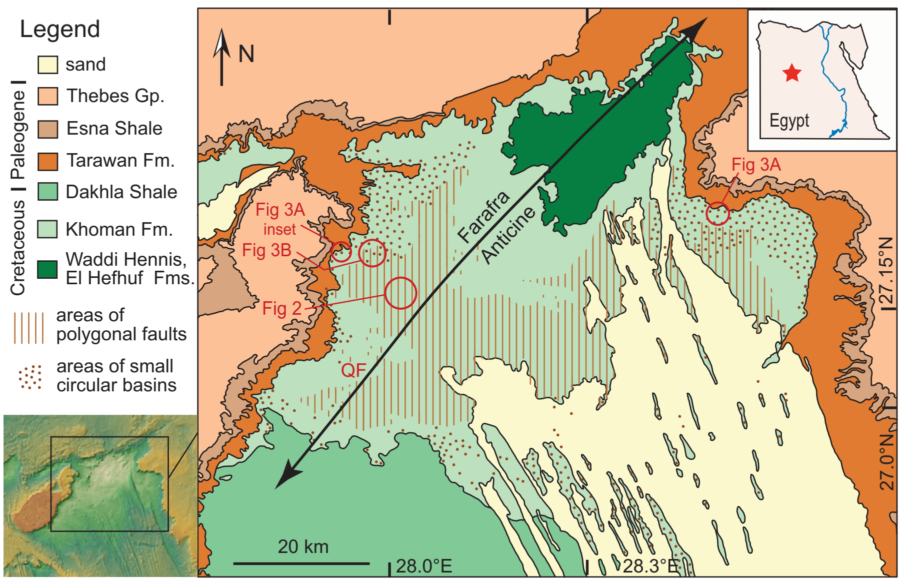

Figure 1. Geologic map showing areas of Khoman Formation that display polygonal faults and small circular structures. QF—Qasr Farafra. Regional geology is adapted from Klitzsch et al. (1987). Inset shaded relief map was developed from Shuttle Radar Topography Mission DEM data.

GEOLOGY, June 2014; v. 42; no. 6; p. 479–482; Data Repository item 2014165 | doi:10.1130/G35362.1 | Published online 15 April 2014

low fault dips in more deeply buried systems (Cartwright, 2011). Berndt et al. (2003) argued for long-term fluid flow over millions of years in the Vøring Basin, with multiple events related to progressive evolution of the underlying polygonal fault system. Polygonal faults are potential fluid conduits (Cartwright et al., 2003), and fluid escape pipes and seafloor pockmarks have been documented in sequences both within (Andresen and Huuse, 2011) and overlying polygonal faults (e.g., Berndt et al., 2003; Gay et al., 2004).

The mechanism of polygonal fault formation remains unclear. Early models involving density inversion, syneresis, and low coefficients of sliding friction along fault planes (e.g., Cartwright et al., 2003; Goulty, 2002) have been joined by models invoking diagenesis (e.g., Davies et al., 2009; Shin et al., 2008; Cartwright, 2011). To date, no consensus model has emerged.

FAULT NETWORK IN THE KHOMAN FORMATION

Our study area lies in massive white chalk of the Late Cretaceous Khoman Formation, exposed in the core of the broad regional Farafra anticline (Fig. 1). The low relief of the wide, flat-floored Farafra Valley coupled with extremely low limb dips (2°–3°) of the Farafra anticline (Omara et al., 1970) combine to create widespread bedding surface exposures over hundreds of square kilometers. The chalk is fine-grained, soft to medium-hard, and moderately consolidated with no clay insoluble residue, siliceous microfossils or macrofossils, quartz veins, or chert.

Exposures of the chalk display narrow resistant fins 10–50 cm high, consisting of calcite veins and vein complexes developed along faults with steep dips (70° to nearly 90°) (Figs. 2A and 2B; see also Figs. DR1–DR3 in the GSA Data Repository[1]). The host chalk is strongly grooved along the fault surfaces (Fig. 2C), and rakes of 80°–90° indicate dip slip. Fault dip direction combined with rare offsets of planar features indicates normal slip (2–3 m calculated for the fault in Fig. 2D).

Veins range in thickness up to 25 cm and consist of coarse calcite crystals both parallel and perpendicular to fault surfaces, commonly extending into dilatant space. The veins create casts of preexisting strongly grooved fault surfaces in the chalk (Fig. 2E; Figs. DR4 and DR5). Calcite veins commonly exhibit multiple phases, some with slivers of chalk between veins. Damage zones within the host chalk are narrow (5–10 cm) and are characterized by fractures of multiple orientations filled by thin calcite veins. The chalk also hosts very thin (1–2 mm) planar goethite veins that lack grooves and slickenlines and that were likely originally iron sulfide (pyrite or marcasite). Iron sulfide (now goethite) also occurs as crystal clusters, veneers, and masses within some calcite veins. Isotopic analyses from a small number of calcite vein and host rock samples suggest reequilibration of formation-generated (marine calcite) fluids with isotopically light meteoric waters (for methods and data, see the Data Repository).

The overall organization of faults is spectacularly revealed in high-resolution satellite images. Faults are arranged in clusters of 5–20 quasi-parallel normal faults and fault segments that define polygonal areas 500–1000 m across, with fewer faults in the polygon cores (Figs. 2F and 2G; Fig. DR6). Faults show no regional preferred orientations (Fig. 2H), although rare faults cut across multiple polygons (arrow, Fig. 2G). Polygon corners are complex interaction zones containing multiple fault orientations with inconsistent crosscutting relationships that imply overlap in the timing of their growth (Fig. 2I; Fig. DR7), as well as arcuate faults that gradually curve from one side into an adjacent side of the polygon. These features imply simultaneous activity of normal faults with distinctly different strikes and no dominant extension direction.

The polygonal network of faults in the Farafra Valley is confined to the Khoman Forma-

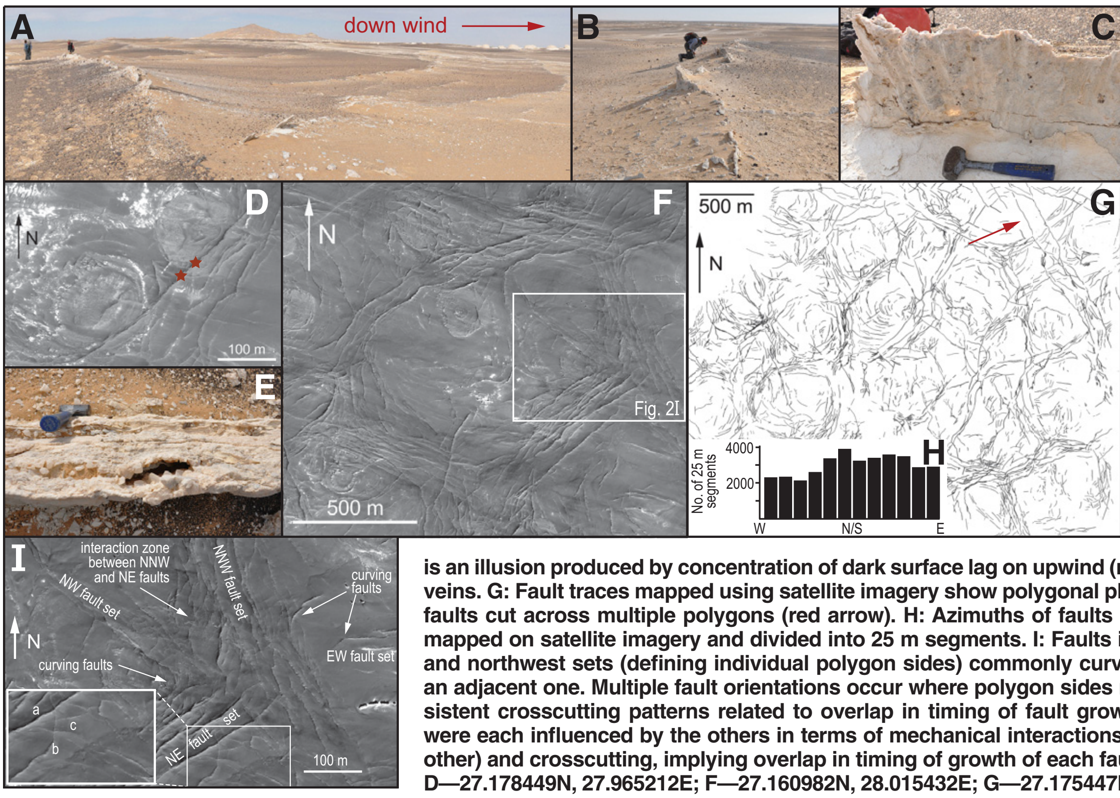

Figure 2. A–C: Low, strongly grooved, coarse calcite veins mark faults in chalk. Rock hammer in C is 27 cm long. D: Throw calculated from field measurements (at stars) on prominent fault in polygon-bounding cluster is 2–3 m. E: Multiphase veins with calcite crystallized in dilatant space, forming casts of grooves along fault surfaces. Rock hammer head is 9 cm long. F: Faults are arranged in clusters that border polygonal areas with lower fault density. Faults appear to be prominent ridges in satellite imagery (illumination from southeast). Field exposures (in A) show that this is an illusion produced by concentration of dark surface lag on upwind (northwest) sides of low calcite veins. G: Fault traces mapped using satellite imagery show polygonal plan view of fault clusters. Rare faults cut across multiple polygons (red arrow). H: Azimuths of faults in representative 25 km² area mapped on satellite imagery and divided into 25 m segments. I: Faults in north-northwest, northeast, and northwest sets (defining individual polygon sides) commonly curve from one polygon side into an adjacent one. Multiple fault orientations occur where polygon sides meet and interact, with inconsistent crosscutting patterns related to overlap in timing of fault growth. Insets: Faults a, b, and c were each influenced by the others in terms of mechanical interactions (curving of one fault into another) and crosscutting, implying overlap in timing of growth of each fault orientation. Image centers: D—27.178449N, 27.965212E; F—27.160982N, 28.015432E; G—27.175447N, 28.010321E; I—27.160073N, 28.020536E. Images D, F, and I are DigitalGlobe WorldView I satellite images (www.digitalglobe.com/). Also see Figures DR1–DR7 (see footnote 1).

[1]GSA Data Repository item 2014165, supplementary methods, and Figures DR1–DR11, is available online at www.geosociety.org/pubs/ft2014.htm, or on request from editing@geosociety.org or Documents Secretary, GSA, P.O. Box 9140, Boulder, CO 80301, USA.

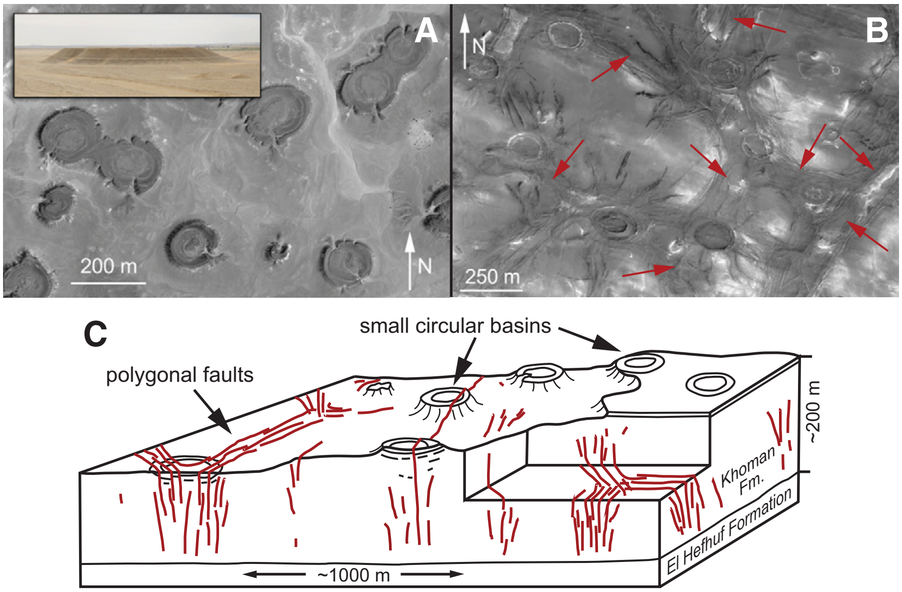

Figure 3. A: Small mesas capped by inward-dipping layers. Inset shows mesa profile. B: Low-relief circular structures with inward-dipping layers and radial rays of calcite and iron oxide (originally iron sulfide) veins; circular structures are spatially associated with polygon-bounding fault clusters (arrows). C: Schematic representation of faults and small basins in Khoman Formation at current level of erosion. Image centers: A—27.289982N, 28.491490E; inset is located at 27.230642N, 27.930565E; B—27.221490N, 27.976172E. Images A and B are DigitalGlobe WorldView I satellite images (www.digitalglobe.com/). Also see Figures DR8–DR11 (see footnote 1).

tion, which is at least 220 m thick (Barakat and Hamid, 1974). The faults die out almost entirely in the uppermost part of the Khoman Formation and are absent in the underlying El Hefuf and Wadi Hennis Formations (Fig. 1).

SMALL CIRCULAR BASINS

The upper part of the Khoman Formation is characterized by more than 2000 isolated small circular basins 50–200 m in diameter, spaced 200–500 m apart, and with inward dips of 5°–20° (Figs. 1 and 3). The circular basins highest in the section form small mesas <10 m high capped by an inward-dipping resistant limestone layer (Fig. 3A; Fig. DR8). Basins slightly lower in the section lack both resistant caprock and topographic relief. Some low-relief basins occur in strong spatial association with polygon boundaries and triple junctions (Fig. 3B; Fig. DR9), are cut by normal faults, and display radial vertical veins of calcite and goethite (originally pyrite or marcasite) (Fig. DR10).

Figure 3C shows the spatial relationship among faults, low-relief basins, and basin-capped mesas (Fig. DR11). Most of the small circular basins lie stratigraphically above the fault network, although rare faults with grooved, multiphase calcite veins extend upward through the basin-capped mesas, which are highest in the section.

DISCUSSION

We propose that the Khoman Formation displays the first extensively exposed occurrence of polygonal faults and related fluid flow features to be described on land. Faults are layer-bound normal faults clustered in a linked polygonal network at scales typical for polygonal faults (Cartwright, 2011) and formed in a strain field with no dominant extension direction. We also propose that the small circular basins overlying the polygonal fault system are fluid escape features related to polygonal faulting. The basins are similar in size (100–200 m) to fluid escape pipes and seafloor pockmarks that overlie polygonal fault systems (e.g., Berndt et al., 2003; Gay et al., 2004) and that have been attributed to long-term fluid flow and vertical stacking of pockmarks as sedimentary layers accumulate (Moss and Cartwright, 2010).

Our observations suggest an intimate relationship between fluids and polygonal faults in the Khoman Formation, supported mechanically using Mohr-Coulomb failure considerations. The very steep fault dips (~80°) indicate that shear failure occurred under conditions where the Mohr circle intersected the failure envelope where σ_3 was negative (tensile), but had not reached the tensile strength of the rock. This condition was most likely achieved by driving a small Mohr circle (with maximum shear stress less than the rock cohesion) to the left by increasing pore fluid pressure. In contrast, a σ_3 decrease caused solely by syneresis or diagenetic volume decrease with a constant σ_1 would have resulted in an expanding Mohr circle intersecting the failure envelope at positive σ_3, unless σ_1 were very small. Resultant faults would have dips of ~60°, which is not what we observe.

Elevated pore fluid pressure played a prominent role in early models for polygonal fault initiation (e.g., Henriet et al., 1991; Cartwright, 1994; Cartwright and Lonergan, 1996). Recent attention has shifted to diagenetic models to account for the significant volumetric strain involved in polygonal fault formation (e.g., Davies et al., 2009; Shin et al., 2008; Cartwright, 2011). The absence of any evidence for silica and clay in the Khoman Formation, however, indicates that a model of fault initiation by volume loss due to diagenesis of biogenic silica (Davies et al., 2009) or smectite (Cartwright, 2011) is neither applicable nor necessary to account for polygonal faulting. For polygonal faults in the Khoman Formation, we therefore conclude that pore fluid pressure played an important role in fault initiation and subsequent activity. The origin of these fluid pressures is unknown, but could reasonably be linked to the compaction and induration of sediments during burial.

Once faults formed, repeated fluid flow events clearly utilized the faults as conduits, forming vein systems. Although we have no unequivocal evidence for the timing of fluid flow and vein mineralization, our isotopic data permit vein formation as polygonal faults evolved (see the Data Repository). One possibility is that creation of steep fault surfaces enabled subsequent slip events to occur under hybrid dilational/shear conditions, with euhedral calcite crystallizing in dilational space as casts of grooved fault surfaces. As each slip event dilated the fault further, new veins would have formed alongside older ones. Alternatively, all veins may have postdated faulting, with high fluid pressures causing episodic dilation and vein formation along existing, steep fault surfaces. Whichever timing relationship is correct, simultaneous dilation occurred in multiple directions, evidenced by numerous T intersections along fault and vein systems.

Small circular basins cut by polygonal faults in the Khoman Formation, along with sets of basins with strong spatial correlation to polygon boundaries and junctions (Fig. 3C), suggest that polygonal faults grew upward over time through basins formed earlier. The radial geometry of veins around some of the low-relief circular basins spatially associated with polygonal faults (Fig. 3B) is consistent with radial fracturing caused by high transient fluid pressures around a fluid escape pipe in a horizontally isotropic stress field. If true, this relationship may favor a model in which high fluid pressures and flow events along faults occurred coeval with fault activity.

CONCLUSIONS

The Khoman Formation hosts extensive exposures of polygonal faults and related fluid flow features, with macroscopic characteristics compatible with polygonal fault systems known from the marine environment. Our field observations reveal small-scale features that were previously unknown, such as tight fault clusters within contemporaneously developing polygon arms, extensive vein systems, and slip indicators. Steep fault dips and abundant vein systems suggest an intimate relationship between pressurized fluids and faulting during both initial mechanical failure of the chalk and the subsequent evolution of the system. Our field observations provide new insights into these polygonal fault systems in marine environments and may assist in the recognition of on-land exposures elsewhere.

ACKNOWLEDGMENTS

This study was supported by funding from the National Science Foundation (grants 1030224 and 1030230) and Hamilton College (New York, USA). Imagery was supplied by the Polar Geospatial Center (Minnesota, USA). We gratefully acknowledge mapping by Joseph Coons, Eric Doubet, David Saint-Jacques, and Carolyn Tewksbury-Christle, and isotopic analyses by Anthony Haigh and Jacob Vincent, and Andrea Lini of the University of Vermont Environmental Stable Isotope Laboratory. Careful reviews and thoughtful commentary by editor Robert Holdsworth and reviewers Ian Alsop, Joseph Cartwright, and Mads Huuse greatly improved the manuscript.

REFERENCES CITED

Andresen, K.J., and Huuse, M., 2011, 'Bulls-eye' pockmarks and polygonal faulting in the Lower Congo Basin: Relative timing and implications for fluid expulsion during shallow burial: Marine Geology, v. 279, p. 111–127, doi:10.1016/j.margeo.2010.10.016.

Barakat, M., and Hamid, M., 1974, Subsurface geology of Farafra Oasis, Western Desert: Egyptian Journal of Geology, v. 17, p. 97–110.

Berndt, C., Bünz, S., and Mienert, J., 2003, Polygonal fault systems on the mid-Norwegian margin: A long-term source for fluid flow, *in* Van Rensbergen, P., et al., eds., Subsurface sediment mobilization: Geological Society of London Special Publication 216, p. 283–290, doi:10.1144/GSL.SP.2003.216.01.18.

Cartwright, J.A., 1994, Episodic basin-wide fluid expulsion from geopressured shale sequences in the North Sea: Geology, v. 22, p. 447–450, doi:10.1130/0091-7613(1994)022<0447:EBWFEF>2.3.CO;2.

Cartwright, J., 2011, Diagenetically induced shear failure of fine-grained sediments and the development of polygonal fault systems: Marine and Petroleum Geology, v. 28, p. 1593–1610, doi:10.1016/j.marpetgeo.2011.06.004.

Cartwright, J., and Dewhurst, D., 1998, Layer-bound compaction faults in fine-grained sediments: Geological Society of America Bulletin, v. 110, p. 1242–1257, doi:10.1130/0016-7606(1998)110<1242:LBCFIF>2.3.CO;2.

Cartwright, J.A., and Lonergan, L., 1996, Volumetric contraction during the compaction of mudrocks: A mechanism for the development of regional-scale polygonal fault systems: Basin Research, v. 8, p. 183–193, doi:10.1046/j.1365-2117.1996.01536.x.

Cartwright, J., James, D., and Bolton, A., 2003, The genesis of polygonal fault systems: A review, *in* Van Rensbergen P., et al., eds., Subsurface sediment mobilization: Geological Society of London Special Publication 216, p. 223–243, doi:10.1144/GSL.SP.2003.216.01.15 .

Davies, R., Ireland, M., and Cartwright, J., 2009, Differential compaction due to the irregular topology of a diagenetic reaction boundary: A new mechanism for the formation of polygonal faults: Basin Research, v. 21, p. 354–359, doi:10.1111/j.1365-2117.2008.00389.x.

Gay, A., Lopez, M., Cochonat, P., and Sermondadaz, G., 2004, Polygonal faults-furrows system related to early stages of compaction—Upper Miocene to recent sediments of the Lower Congo Basin: Basin Research, v. 16, p. 101–116, doi:10.1111/j.1365-2117.2003.00224.x.

Goulty, N.J., 2002, Mechanics of layer-bound polygonal faulting in fine-grained sediments: Geological Society of London Journal, v. 159, p. 239–246, doi:10.1144/0016-764901-111.

Hansen, D., Shimeld, J., Williamson, M., and Lykke-Andersen, H., 2004, Development of a major polygonal fault system in Upper Cretaceous chalk and Cenozoic mudrocks of the Sable Subbasin, Canadian Atlantic Margin: Marine and Petroleum Geology, v. 21, p. 1205–1219, doi:10.1016/j.marpetgeo.2004.07.004.

Henriet, J.P., Batist, M.D., and Verschuren, M., 1991, Early fracturing of Paleogene clays, southernmost North Sea: Relevance to mechanisms of primary hydrocarbon migration, *in* Spenser, A.M., ed., Generation, accumulation and production of Europe's hydrocarbons: European Association of Petroleum Geologists Special Publication 1, p. 217–227.

Hibsch, C., Cartwright, J., Hansen, D., Gaviglio, P., André, G., Cushing, M., Bracq, P., Juignet, P., Benoit, P., and Allouc, J., 2003, Normal faulting in chalk: Tectonic stresses vs. compaction-related polygonal faulting, *in* Van Rensbergen, P., et al., eds., Subsurface sediment mobilization: Geological Society of London Special Publication 216, p. 291–308, doi:10.1144/GSL.SP.2003.216.01.19 .

Klitzsch, E., List, F.K., and Pöhlmann, G., 1987, Geological map of Egypt NG3 35 NE Farafra: Cairo, Egypt, Conoco Coral and Egyptian General Petroleum Company, scale 1:500,000.

Moss, J., and Cartwright, J., 2010, 3D seismic expression of km-scale fluid escape pipes from offshore Namibia: Basin Research, v. 22, p. 481–501, doi:10.1111/j.1365-2117.2010.00461.x.

Omara, S., Hemida, I., and Sanad, S., 1970, Structure and hydrogeology of Farafra Oasis, Western Desert, U.A.R.: Seventh Arab Petroleum Congress, Kuwait, Paper 65, p. 15.

Shin, H., Santamarina, J.C., and Cartwright, J.A., 2008, Contraction-driven shear in compacting uncemented sediments: Geology, v. 36, p. 931–934, doi:10.1130/G24951A.1.

Verschuren, M., 1992, An integrated 3D approach to clay tectonic deformation and the development of a new 3D surface modelling method [Ph.D. thesis]: Ghent, Belgium, Universiteit Gent, 359 p.

Manuscript received 8 December 2013
Revised manuscript received 2 March 2014
Manuscript accepted 4 March 2014

Printed in USA